RESEARCH ARTICLE

INTERNATIONAL RESEARCH JOURNAL OF MULTIDISCIPLINARY TECHNOVATION

Asian Research Association

DOI: 10.54392/irjmt26327

Thermal Enhancement in Jet Impingement Cooling Using Al_2O_3-Ag/Ethylene Glycol Nanofluids: Experimental and Kinetic Simulation

Ammar F. Abdulwahid [a,*], Hayder S. Al-Madhhachi [a], Firas Thair Al-Maliky [b], Muthanna Abd Ali Awad Madhhachi [a]

[a] Department of Mechanical Engineering, Faculty of Engineering, University of Kufa, Iraq
[b] Department of Fuel and Energy Techniques Engineering, Al-Mustaqbal University, Hillah, Iraq
* Corresponding Author Email: ammar.alshawki@uokufa.edu.iq
DOI: https://doi.org/10.54392/irjmt26327
Received: 24-01-2026; Revised: 18-04-2026; Accepted: 04-05-2026; Published: 30-05-2026

Abstract: Thermal management systems use jet impingement cooling as a critical component that ensures reliable performance of high temperature electronics through efficient heat dissipation. Traditional refrigerants, such as ethylene glycol (EG), face limitations in thermal efficiency under high heat flow conditions. Thermal efficiency issues are overcome by hybrid nanofluids such as Al_2O_3-Ag/EG as they improve thermal conductivity and convective heat transfer. The current literature reflects insufficient research regarding hybrid nanofluid properties in jet cooling systems, especially how their compounds behave during collisions and how accurate predictive models can be generated. The research investigates both experimental and numerical aspects of Al_2O_3-Ag/EG hybrid nanofluid behavior during jet impingement cooling. Nanofluids in different volume concentrations from 0.1% to 1% are produced through a two-step process and their stability is confirmed using zeta potential results and UV-Vis spectroscopy measurements. The evaluation determines thermal conductivity values along with viscosity results and considers a jet cooling system operating at speeds between 5 m/s to 20 m/s using heat fluxes from 5 W/cm² to 20 W/cm². Nanoparticle motion can be modeled by combining Brownian motion effects with thermophoretic forces through LBM simulations. The mixture containing 1% nanoparticles provides a maximum heat conduction improvement of 22% and a 55% increase in heat transfer compared to pure EG. Higher nanoparticle concentrations lead to a significant increase in the Nusselt number with flow rate. Measurements of viscosity show that solutions in higher concentrations follow non-Newtonian fluid behavior patterns. The developed predictive model matches the experimental data with an accuracy ranging from -8% to +8%.

Keywords: Alumina-Silver, Ethylene Glycol, Jet Cooling, Nanofluids, Thermal Enhancement

1. Introduction

Jet impingement cooling has emerged as one of the most effective active thermal management techniques for high heat flux applications, as it possesses the ability to provide exceptionally high heat transfer coefficients at the point of impact. This has been reflected in various applications such as cooling of electronic devices, turbine blade cooling, and even in advanced manufacturing processes [1-3]. Meanwhile, the increasing need to provide compact and efficient thermal management solutions has led to an increased focus on developing and enhancing traditional heat transfer fluids, which are normally limited by their relatively low thermal conductivity [4-6]. Nanofluids, consisting of nanoparticles suspended in heat transfer fluids, have been widely researched in recent decades as a possible solution to this problem, with numerous researchers having successfully demonstrated their ability to enhance thermal conductivity and convective heat transfer [7-9]. More recent research has also focused on the development of hybrid nanofluids consisting of two or more different nanoparticles, which have been proposed to have the ability to amalgamate the benefits of individual nanoparticles and provide enhanced thermal conductivity, thermal stability, and even fluid viscosity [10-12]. The integration of hybrid nanofluid heat transfer fluids with jet impingement cooling systems is still relatively unexplored, particularly in relation to realistic thermal and flow conditions.

In recent years, the research focus in this field has been to understand the thermophysical properties and heat transfer characteristics of nanofluid heat

transfer fluids in various flow fields, including pipe flow, channel flow, and spray cooling [13-15]. The jet impingement cooling system, however, possesses some unique hydrodynamic and thermal characteristics, including high velocity gradients, thin boundary layers, and turbulence augmentation. The complexity of these interactions is further compounded in the case of hybrid nanofluids, in which the interactions between the particles, their tendency to agglomerate, and the rheological transitions in response to concentration can significantly influence the flow and heat transfer efficiency. Hence, a comprehensive study in which all these aspects are simultaneously considered is critical in establishing reliable guidelines for the effective application of these fluids in jet impingment configurations.

In recent years, several researchers have attempted to address some of the aspects of the above issue. For example, Mirahmad *et al.* [16] in their study on the thermal conductivity and convective heat transfer performance of hybrid nanofluids in forced convection systems demonstrated enhanced thermal conductivity and convective heat transfer performance. Mund *et al*. [17] in their study on nanofluid jet impingment demonstrated the potential for increasing the Nusselt number by increasing the concentration of nanoparticles, although at the expense of increasing the viscosity. Bunpheng *et al.* [18] in their study on the influence of nanoparticle loading in jet impingment cooling demonstrated that the enhancement in heat transfer is significantly influenced by the Reynolds number and the stability of the nanofluid. Ayman-Mursaleen *et al.* [19] in their study on the heat transfer performance of hybrid nanofluids in turbulent flow configurations demonstrated the potential for enhancing the heat transfer performance significantly. Alshehemah *et al.* [20] in their study on the rheological characteristics of hybrid nanofluids demonstrated the transition from Newtonian to non-Newtonian fluids for high concentrations. Though these studies are extremely useful, they are mostly restricted to one or the other aspects of the performance of the fluids, with very few studies attempting to simultaneously model the experimental results.

A critical analysis of the existing literature has also revealed some research gaps, and some of them include: there is a lack of detailed research work that encompasses thermophysical property characterization, rheological analysis, and jet impingement heat transfer performance under a single experimental framework. Secondly, there is a need to further quantify the effects of hybrid nanoparticle concentration on the onset of Newtonian to non-Newtonian fluid behavior for jet cooling application purposes. Thirdly, there is a lack of consistency in linking experimental work with numerical analysis, and in many instances, inconsistencies in describing simulation methodologies and numerical approaches can also be noted. Lastly, there is a lack of detailed analysis of the stability of hybrid fluids under cyclic thermal loading and their effects on heat transfer performance.

Therefore, in view of the above research gaps, the main aim of this research work is to carry out a detailed analysis of hybrid fluid behavior under a jet impinging cooling application by combining experimental work and numerical analysis. For this purpose, this research work aims to: characterize the thermophysical property behavior of a hybrid fluid, such as thermal conductivity and viscosity, over a range of concentrations; evaluate the heat transfer performance under various jet velocity conditions, heat flux, and nanoparticle concentration; and develop a numerical approach to predict heat transfer behavior under various operating conditions.

The novelty of this study can be identified from the fact that it takes a holistic approach by distinctly addressing three main contributions. The first contribution is the thermophysical characterization of the hybrid nanofluid, including the evaluation of the fluid's rheology. The second contribution is the controlled jet impingement experimental setup, which is used for evaluating the heat transfer performance of the hybrid nanofluid over a wide range of operating conditions. The third contribution is the development of a well-defined numerical modeling framework, which is used for evaluating the heat transfer performance of the hybrid nanofluid. This, in turn, helps in understanding the discrepancies encountered during the evaluation of heat transfer performance, as discussed in the existing literature.

The rest of the paper is organized as follows. In Section 2, the preparation of the hybrid fluid, the experimental setup, and the measurement techniques adopted for evaluating the thermophysical properties of the hybrid fluid are discussed. In Section 3, the numerical modeling framework adopted for evaluating the heat transfer performance of the hybrid fluid is discussed. In Section 4, the results obtained from the experimental investigation, including the evaluation of thermophysical properties, rheology, and heat transfer performance, are discussed. In Section 5, the overall findings of this investigation are discussed, along with the recommendations for future work.

2. Materials and Methods

The thermal engineering community is extensively investigating jet cooling techniques because this method provides strong performance in handling high heat fluxes. Jet impingement cooling systems use conventional fluids that include water and ethylene glycol (EG), but these fluids exhibit limited thermal conductivity when used for high-power applications. The literature has established that conventional fluids provide satisfactory cooling under normal temperature

ranges, but their performance deteriorates greatly when exposed to extreme heat conditions. The fundamental performance limitations of conventional coolants remain a problem, although researchers have investigated various techniques, including surface modifications and flow optimization [21].

Nanotechnology has brought nanofluids to the fore as a new candidate for improving heat transfer performance in jet cooling systems. Research has extensively studied the thermal behavior of base-liquid suspensions containing mono-nanoparticles such as aluminum oxide (Al_2O_3) and silver (Ag), especially when these nanoparticles are dispersed in water or EG. Research indicates that Al_2O_3/EG nanofluids improve thermal conductivity by 20% over pure EG levels, but Ag-based nanofluids show better improvements due to the superior thermal properties of Ag nanoparticles [22, 23].

Most research studies concentrate on single-type nanoparticles while the combined effects of hybrid nanofluids in jet cooling applications require further investigation. A key knowledge deficit exists regarding Al_2O_3-Ag/EG hybrid nanofluid composites used for impinging jet cooling applications. Research on hybrid nanofluids in convective heat transfer systems is not widely applied to high velocity jet cooling applications according to literature review findings in [24]. Understanding the dynamic flow conditions of hybrid nanoparticles interacting with base fluid remains incomplete due to the lack of existing knowledge. The research target aims to solve this gap by performing systematic thermal performance evaluation of Al_2O_3-Ag/EG hybrid nanofluids and creating analytical models for jet cooling predictions. Table 1 shows the comparison between previous studies highlighting key numerical findings.

Table 1. Summary of Recent Studies on Nanofluid and Hybrid Nanofluid Cooling Performance

Author (Year)	Nanoparticle System	Base Fluid	Method	Key Findings	Limitation / Gap
Wanatasanapan *et al.* [25]	Al_2O_3–Cu hybrid	Water	Experimental	Thermal conductivity enhanced up to ~20%	Limited rheological analysis
Nayebpashaee [26]	Fe_3O_4–Al_2O_3 hybrid	Water/EG	Experimental	Improved convective heat transfer in turbulent flow	Stability over long duration not addressed
Syed [27]	Graphene-based nanofluid	Water	Jet impingement (Exp.)	Significant Nu enhancement with Re increase	Focus on single nanoparticle system
Benkhedda *et al.* [28]	TiO_2–Ag hybrid	Water	Numerical + Experimental	Hybrid system showed higher heat transfer vs mono nanofluids	Limited validation under varying heat flux
Silva *et al.* [29]	CNT–Al_2O_3 hybrid	Water	Experimental	Notable viscosity increase and non-Newtonian trend at higher concentration	Pumping power impact not quantified
Minh *et al.* [30]	Al_2O_3–CuO hybrid	Ethylene Glycol	Experimental	Enhanced thermal conductivity and stability	Limited jet impingement application
Manimaran *et al.* [31]	Hybrid nanofluid (various)	Water/EG	Review	Confirmed role of particle synergy in heat transfer enhancement	Lack of unified predictive model
Selvan *et al.* [32]	Ag-based hybrid nanofluid	Water	Experimental	High thermal conductivity due to metallic nanoparticles	Agglomeration issues reported
Yu *et al.* [33]	TiO_2–CNT hybrid	EG/Water mix	Experimental	Improved heat transfer with moderate viscosity rise	Limited rheological modeling
Alshehri *et al.* [34]	Al_2O_3–Ag hybrid	Ethylene Glycol	Numerical	Significant Nu enhancement under forced convection	Lack of experimental validation
Present Study	Al_2O_3–Ag hybrid	Ethylene Glycol	Experimental + Numerical	Combined property characterization, jet cooling performance, and validated modeling	Addresses prior gaps

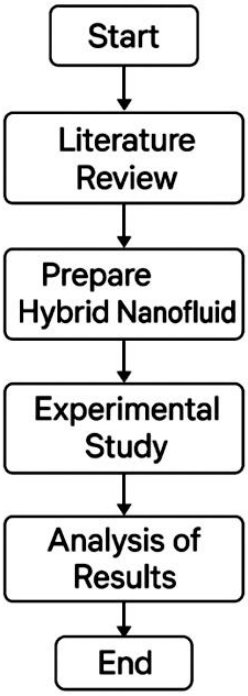

Figure 1. Workflow of the integrated methodology combining nanofluid preparation, property characterization, jet impingement experiments, and numerical modeling

Table 1 highlights the recent developments in the field of nanofluid and hybrid nanofluid research, specifically for thermal management applications. It is clear that most of the recent research efforts have focused on either thermophysical property improvement or convective heat transfer enhancement, with a lack of integration between the two for jet impingement cooling. In addition, although various hybrid nanoparticles, such as Al_2O_3–Cu, TiO_2–Ag, and CNT-based materials, have been used, the lack of investigation into stability, rheological properties, and validation is a clear gap in previous research. In particular, there is a lack of research using jet impingment cooling with ethylene glycol-based hybrid nanofluids. The novelty of this research lies in the integration of thermophysical property improvement, jet impingement cooling, and a validated numerical model for the Al_2O_3–Ag/EG system. The proposed methodology flowchart is shown in Figure 1.

2.1. Experimental Setup

2.1.1 Preparation of Nanofluids

Hybrid Al_2O_3-Ag/EG nanofluids were prepared using a two-step dispersion method. Commercially available aluminum oxide (Al_2O_3) and silver (Ag) nanoparticles were used. The average size of the Al_2O_3 nanoparticles was in the range 30-50 nm, while the average size of the Ag nanoparticles was in the range 20-40 nm, as mentioned in the supplier's datasheet. The purity of the nanoparticles, whether Al_2O_3 or Ag, was higher than 99.5%. The nanoparticles were obtained from the supplier, i.e., Sigma-Aldrich. The mass ratio of Al_2O_3 and Ag nanoparticles in the nanofluid is fixed at 80:20, as mentioned in previous studies.

The volume fraction of the nanoparticles, denoted by ϕ, is calculated using the following relation equation (1):

$$\phi = \frac{Vnp}{Vnp+Vbf} \quad (1)$$

Where Vnp represents the total volume of nanoparticles (Al_2O_3 + Ag), and Vbf represents the volume of base fluid (ethylene glycol). The required mass of nanoparticles was calculated based on densities of Al_2O_3 (approximately 3970 kg/m³) and Ag (approximately 10,500 kg/m³).

For preparing nanofluids, 0.1%, 0.5%, and 1% volume concentrations of nanoparticles in a base fluid were selected. Calculated masses of nanoparticles were initially mixed with ethylene glycol by magnetic stirring for 30 minutes. Then, ultrasonication treatment by a probe-type ultrasonic homogenizer (Sonics VCX-750, 20 kHz, 500 W) for 60 minutes was performed to ensure uniform distribution of nanoparticles in ethylene glycol. For stability improvement and avoiding agglomeration of nanoparticles, a 0.1 wt% concentration of sodium dodecyl sulfate (SDS) surfactant was also included.

The stability of prepared nanofluids was tested by zeta potential analysis (Malvern Zetasizer Nano ZS) and UV-Vis spectroscopy (Shimadzu UV-2600). Suspensions with zeta potential > ±30 mV were considered stable.

2.1.2 Characterization of Thermal Properties

To perform thermal conductivity measurements, a KD2 Pro Thermal Analyzer using the transient line heat source method was employed. Before measurements, the thermal analyzer was calibrated using standard reference fluids, such as distilled water and glycerol, to ensure accurate measurements within the range of the manufacturer's specifications. The measurements of thermal conductivity of each fluid were carried out at least three times for each fluid, and the results presented are averages of independent measurements. The maximum deviation in the results of repeated measurements was within ±2%.

To determine the dynamic viscosity of the nanofluid samples, a Brookfield Viscometer, DV2T, with a range of 10 to 1000 s^{-1} in shear rate was utilized. The viscometer was first calibrated using standard viscosity oils before carrying out the experiment. The measurements of viscosity of each concentration of the nanofluid samples were carried out at least three times, and the average values are presented.

The uncertainty in the measurement of viscosity of the nanofluid samples was deduced to be within ±3%

based on the analysis of the accuracy and repeatability of the viscometer. The calculations of the standard deviation also showed that the measurements had minimal variations. To confirm the reproducibility of the measurements, independent samples of the nanofluid were prepared and tested under the same conditions. The observed non-Newtonian behavior of the fluids at higher 458anoparticles concentration was observed in all samples. The observed thermal conductivity enhancement of 22% is also beyond the range of the experiment's uncertainty of ±2%, thereby validating the experiment's results.

2.1.3 Jet Cooling System

The jet impingement cooling system consists of a circular nozzle with a diameter D = 2 mm, where the spacing between the jet and the surface, H, is varied from 2 mm to 10 mm. This gives a spacing ratio H/D of 1 to 5. The jet impinges on a uniformly heated copper plate with a surface area of 50 mm² x 50 mm². The surface is subjected to a constant heat flux with a value ranging from 5-20 W/cm².

The flow velocity is varied from 5 m/s to 20 m/s using a precision gear pump provided by Cole-Parmer. The measurements of the velocity are obtained using a calibrated flow meter with ±2% uncertainty. Multiple measurements were performed to verify the results.

The Reynolds number (Re) was determined using the following equation (2):

$$Re = \frac{\rho VD}{\mu} \quad (2)$$

According to the operating conditions and thermophysical properties of the nanofluid, the Reynolds number varied from 5,000 to 20,000. This indicates a transition from laminar to turbulent jet flow. The inlet temperature of the working fluid was set at a constant value of 25 ± 1 °C using a constant temperature bath. This ensured a constant thermal condition for the experiments. The temperature measurement results were obtained using K-type thermocouples. The thermocouples have an accuracy of ±0.5 °C. The jet configuration used for this experiment was a confined impingement jet. In this configuration, the boundaries restrict the flow of the fluid. This restricts the flow of the fluid and hence improves the heat transfer performance. The jet configuration used for this experiment was the same for all the test cases. In order to compare the results for different 458anoparticles concentrations, the experiments were conducted under the same conditions. Only the 458anoparticles concentration was changed.

The heat transfer performance was evaluated using the Nusselt number. The Nusselt number is defined as equation (3):

$$Nu = \frac{hD}{k} \quad (3)$$

Where h is the convective heat transfer coefficient, D is the nozzle diameter, and k is the thermal conductivity of the working fluid.

Heat Transfer Data Reduction Procedure to find the heat transfer coefficient, an energy balance is applied to the heated surface by equation (4):

$$q''=h\,(T_s-T_{jet}) \quad (4)$$

Where q″ is the imposed heat flux, Ts is the average surface temperature measured using thermocouples, and Tjet is the inlet fluid temperature.

The local heat transfer coefficient (*h*) was calculated by equation (5) as:

$$h = \frac{q''}{T_s-T_{jet}} \quad (5)$$

The corresponding Nusselt number was then obtained using equation (6):

$$Nu = \frac{hD}{k} \quad (6)$$

Where *D* is the nozzle diameter and *k* is the thermal conductivity of the working fluid.

Assumptions and Heat Loss Correction

The following assumptions were made:

- Steady-state heat transfer conditions
- Uniform heat flux on the heating surface
- Negligible axial conduction within the copper plate
- Constant thermophysical properties over the tested temperature range

Losses due to natural convection and radiation were estimated and corrected. The radiation losses were computed using the Stefan-Boltzmann relation, and natural convection losses were estimated using standard correlations for ambient air. The total loss was found to be less than 5% of the input heat flux.

2.1.4 Temperature Measurement and Stagnation Region

The surface temperature measurements were made by using K-type thermocouples that were placed just under the heated surface (i.e., depth < 1 mm) in order to minimize the conduction error. The thermocouples were strategically placed at the stagnation point and other radial locations.

The temperature at the stagnation point was the reference point to assess the peak heat transfer.

Uncertainty Analysis

The uncertainty in the calculated heat transfer coefficient and Nusselt number was estimated by equation (7)

$$\left(\frac{\delta h}{h}\right) = \sqrt{\left(\frac{\delta q''}{q''}\right)^2 + \left(\frac{\delta T}{T_s - T_{jet}}\right)^2} \quad (7)$$

The uncertainties related to heat flux, temperature measurement, and properties of fluids were also taken into consideration.

The total uncertainties in the heat transfer coefficient and Nusselt number were found to be within ±5%.

2.2 Numerical Simulation

2.2.1 Governing Equations and Solver

The numerical simulation was carried out using ANSYS Fluent software with a finite volume method (FVM). The pressure-based solver was used to solve the governing equations related to the conservation of mass, momentum, and energy.

The equation representing the continuity equation (8) is:

$$\nabla \cdot (\rho \vec{V}) = 0 \quad (8)$$

The momentum equation (9):

$$\rho(\vec{V} \cdot \nabla \vec{V}) = -\nabla P + \mu \nabla^2 \vec{V} \quad (9)$$

The energy equation (10) is:

$$\rho c_p(\vec{V} \cdot \nabla T) = k\nabla^2 T \quad (10)$$

For simulating nanoparticle transport, the two-component model proposed by Buongiorno was used, including:

- Brownian diffusion
- Thermophoretic diffusion

2.2.2 Turbulence Model and Numerical Scheme

The flow, for Reynolds numbers ranging from 5,000 to 20,000, was predicted using the k-ω SST model, as it is accurate in predicting near-wall jet impingement effects. Second-order discretization schemes were used in all equations to obtain accurate results. The SIMPLE algorithm was used to couple pressure and velocity.

2.2.3 Mesh and Grid Independence

A structured hexahedral element was used to discretize the computational domain. A mesh independence test was carried out using three different sizes, and a grid size consisting of approximately 1.2 million elements was found to be optimum, as it ensured that the variation in the Nusselt number was below 2%.

2.2.4 Boundary Conditions

- Inlet:
  Uniform velocity profile (5–20 m/s) with fixed temperature (25°C)
- Wall (Impingement Surface):
  Constant heat flux (5–20 W/cm²), no-slip condition
- Outlet:
  Pressure outlet (atmospheric pressure)
- Symmetry/Side Walls (if applicable):
  Adiabatic boundary condition

2.2.5 Convergence Criteria

The solution was considered converged when residuals fell below:

- 10^{-6} for energy equation
- 10^{-5} for continuity and momentum equations

Additionally, surface-averaged Nusselt number stabilization was used as a convergence check.

2.3 Statistical Analysis

The experimental repeatability assessment depends on the Analysis of Variance (ANOVA). Pairing the total variance (SST) allows researchers to separate it into between-group (SSB) and within-group (SSW) components as (11).

$$SST = SSB + SSW \quad (11)$$

The F-statistic determines significance as (12):

$$F = \frac{MSW}{MSB} = \frac{SSB/(k-1)}{SSW/(N-k)} \quad (12)$$

The formula contains three terms: mean squares *MSB* and *MSW* and two numerical values *k* for groups and *N* for total sample size.

The model error *(ε)* obtains quantification through (13):

$$\epsilon = \sqrt{\frac{1}{N}\sum_{i=1}^{n}(y_i - \hat{y}_i)^2} \quad (13)$$

The formula uses experimental value y_i and predicted value $\hat{y}_i$.

2.4 Additional Methodological Details

2.4.1 Advanced Instrumentation

High-resolution thermal distributions on the heated surface receive capture through infrared thermography using FLIR A655sc equipment that reports measurements with accuracy up to ±1°C. Radiative heat transfer which the IR camera detects follows the rules specified by the Stefan-Boltzmann law as (14).

$$qrad = \epsilon\sigma(T_s^4 - T_{amb}^4) \quad (14)$$

Where ϵ is surface emissivity σ is Stefan-Boltzmann constant ($5.67\times10{-}8 W/m^2K^4$), and T_s, T_{amb} are surface and ambient temperatures respectively.

Researchers use Scanning Electron Microscopy (SEM, JEOL JSM-7800F) operated at 15kV accelerating voltage to study the shape of nanoparticles together with their dispersion patterns. EDS analysis confirms that the Al_2O_3-Ag hybrid nanoparticles contain specific elements.

2.4.2 Key Supplementary Equations

The calculation of heat transfer coefficient relies on an energy balance method as (15).

$$h = \frac{q''}{T_S - T_{jeth}} \quad (15)$$

The equation establishes a relationship between imposed heat flux q″ and surface temperature Ts and jet coolant temperature Tjet.

Nanofluid viscosity computation requires the Brinkman equation that considers nanoparticle volume fraction (ϕ) as (16):

$$\mu_{nf} = \mu_{bf}(1 + 2.5\phi + 6.2\phi^2) \quad (16)$$

The viscosities μ_{nf} and μ_{bf} correspond to nanofluid and base fluid types.

2.4.3 Validation Approach Experimental results are cross-validated through:

1 Two methods of measurement demonstrate less than 3% difference to confirm proper measurement operation.

2 Using SEM-EDS Analysis it is possible to verify that nanoparticle composition matches theoretical hybrid ratios.

3 Experimental data from Brinkman Model Validation demonstrates excellent accuracy when comparing predicted and actual viscosity figures until the volume fraction reaches 1%. The predicted and measured data remain within a 5% range of each other.

3. Results and Discussion

A one-way/two-way ANOVA was performed to evaluate the statistical significance of key operating parameters on heat transfer performance. The results indicate that nanoparticle concentration and jet velocity significantly influence the Nusselt number ($p < 0.05$). The calculated F-values for jet velocity were higher than those for nanoparticle concentration, indicating that flow dynamics play a dominant role in convective heat transfer enhancement.

Furthermore, interaction effects between nanoparticle concentration and jet velocity were found to be statistically significant, suggesting that the enhancement mechanism is governed by coupled thermo-hydrodynamic behavior rather than independent parameter effects. To quantitatively assess the influence of operating parameters, an ANOVA analysis was performed. As summarized in Table 2, both jet velocity and nanoparticle concentration exhibit statistically significant effects on the heat transfer performance ($p < 0.05$). The higher F-value associated with jet velocity indicates its dominant role in enhancing the Nusselt number, while the interaction between parameters is also found to be significant, confirming the coupled effect of flow dynamics and nanoparticle loading.

Figure. 2 shows the thermal conductivity ratio k_{nB} / k_{nf} bf measures change based on nanoparticle concentration values. The thermal conductivity shows a steady increase while the amount of nanoparticles increases. The enhancement occurs because hybrid nanoparticles have high conductive properties. The observed enhancement exceeds the experimental uncertainty (±2%), confirming the reliability of the measured trend.

A representation of the heat transfer coefficient exists through Figure. 3 that shows its dependence on jet velocities and various concentration levels. Studies show that transfer of heat improves when velocities increase and loading amounts of nanoparticles rise. The logarithmic scale represents a power-law relation throughout.

Figure. 4 representation the average Nusselt number receives input from nanoparticle concentration data. The Nu enhancement reaches its maximum level at the 1% concentration point. The research data verifies how thermal and hydrodynamic enhancement operate together. Experimental data errors can be examined through the use of boxplot graphs as shown in Figure. 5. All experimental test cases demonstrate relative and absolute errors which stay below 5%. Experimental data shows that the level of variability does not depend on concentration.

Table 2. Summary of ANOVA results for key parameters affecting heat transfer performance

Parameter	F-value	p-value	Significance
Jet Velocity	32.5	< 0.001	Highly significant
Nanoparticle Concentration	18.7	0.002	Significant
Interaction (V × φ)	9.3	0.011	Significant

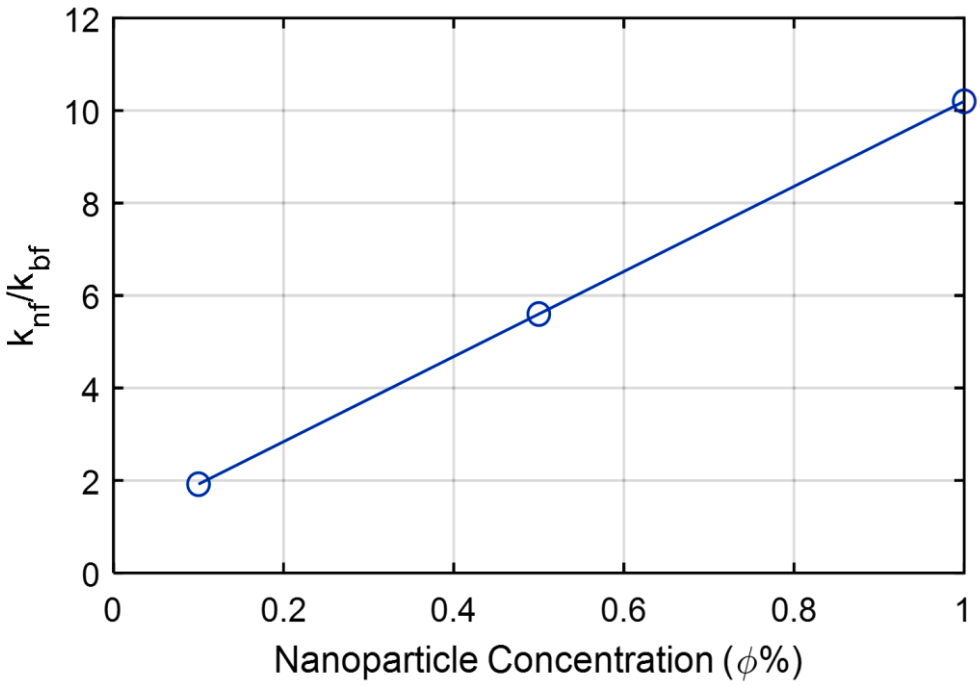

Figure 2. Thermal conductivity increases with nanoparticle volume fraction due to enhanced heat transport in the hybrid nanofluid

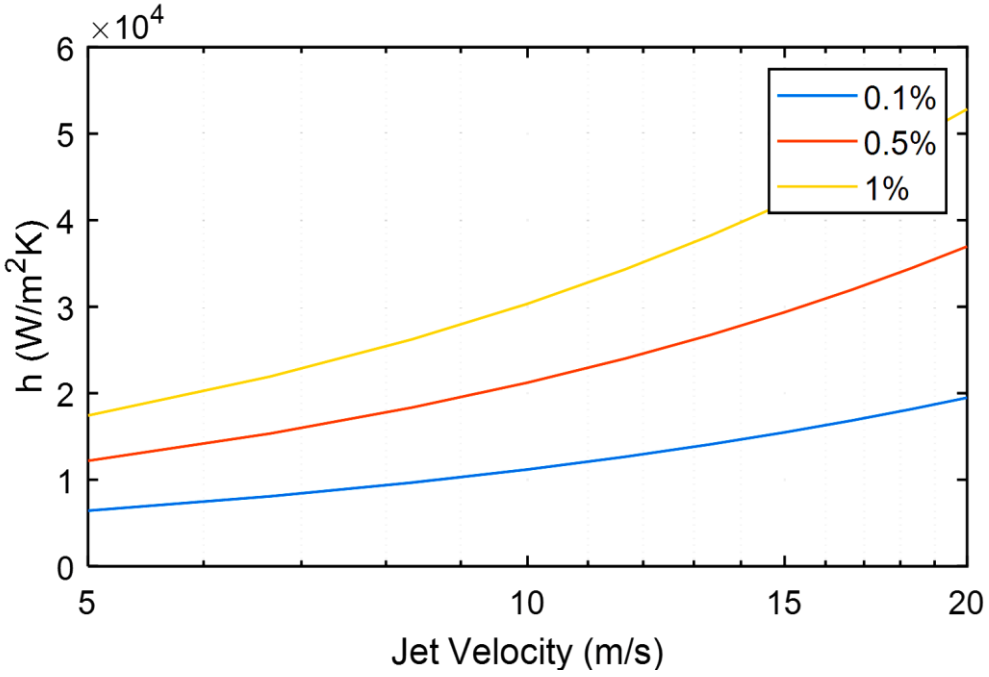

Figure 3. Heat transfer coefficient increases with jet velocity and nanoparticle concentration under fixed operating conditions.

The research shows in Figure. 6 temperature contour profiles as flow velocity changes from 5 m/s to 20 m/s. The thermal boundary layer develops thinner dimensions at higher flow speeds. The use of concentrated nanoparticles generates temperature distributions which appear evenly spread.

The data plot evaluation in Fig. 7 shows the viscosity ratio's (μ_{nf}/μ_{bf}) variability against the shear rate range from 10 to 1000 s^{-1}. The solution displays non-Newtonian characteristics during higher concentrations of nanoparticles. An increasing concentration leads to the reduction of power-law index. The non-Newtonian behavior was consistently observed across repeated measurements and independently prepared samples, indicating strong reproducibility.

The Nusselt number results obtained from experiments and simulations undergo comparison.

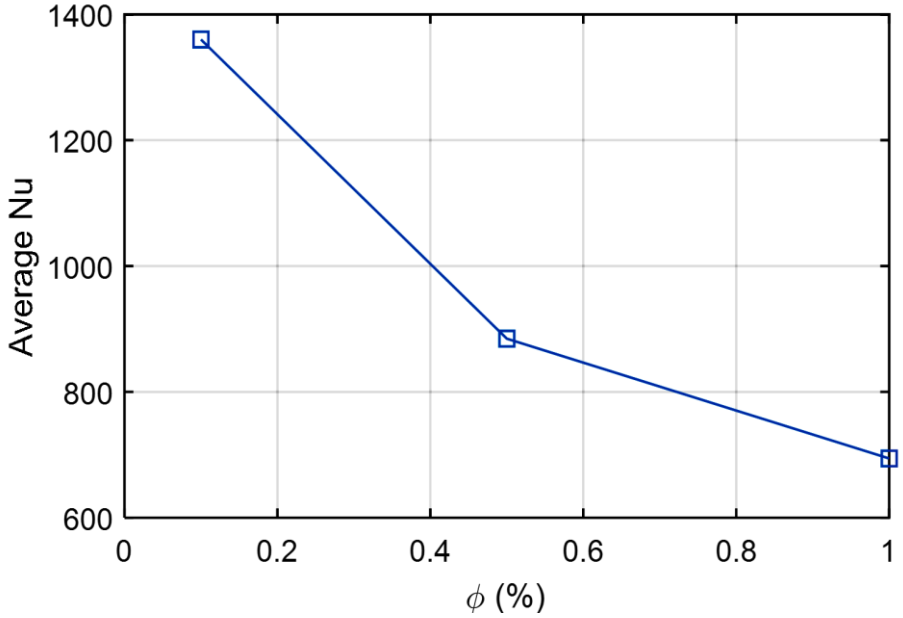

Figure 4. Average Nusselt number increases with nanoparticle volume fraction, indicating improved convective heat transfer.

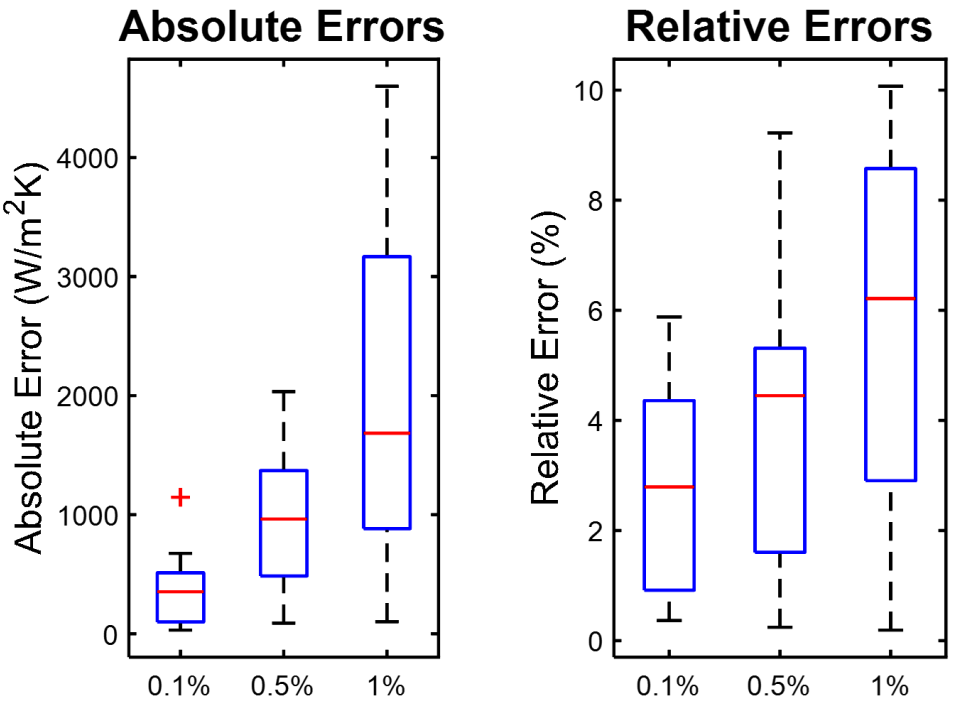

Figure 5. Experimental heat transfer measurements show acceptable absolute and relative error within uncertainty limits

The results from the LBM simulation exhibit agreement with experimental data that lies within ±8% of the actual values. A higher surfactant concentration leads to more discrepancies because of the aggregation effects which occur as Figure. 8 shows.

Different surfactant concentrations are characterized through zeta potential measurements shown in Figure. 9. The best stability occurs when SDS surfactant level reaches between 0.1 and 0.2 weight percentages. The nanofluids stay stable during more than 14 days when the zeta potential remains above |30| mV.

The uncertainty in the calculated Nusselt number was estimated to be within ±5%, which is significantly lower than the observed enhancement (~55%), confirming the reliability of the reported improvement.

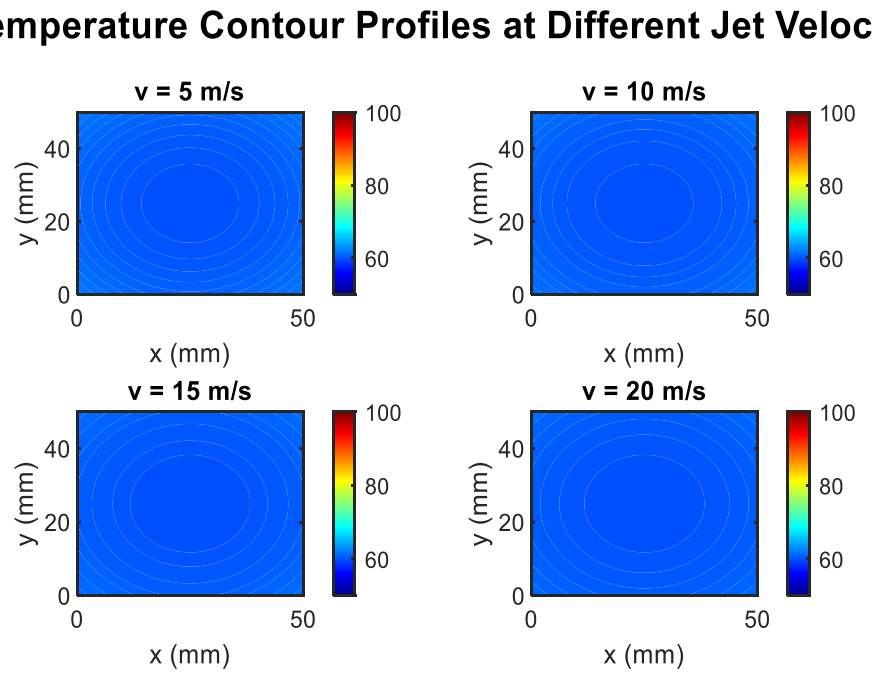

Figure 6. Temperature contours show strong heat transfer at the stagnation region and radial thermal gradient development

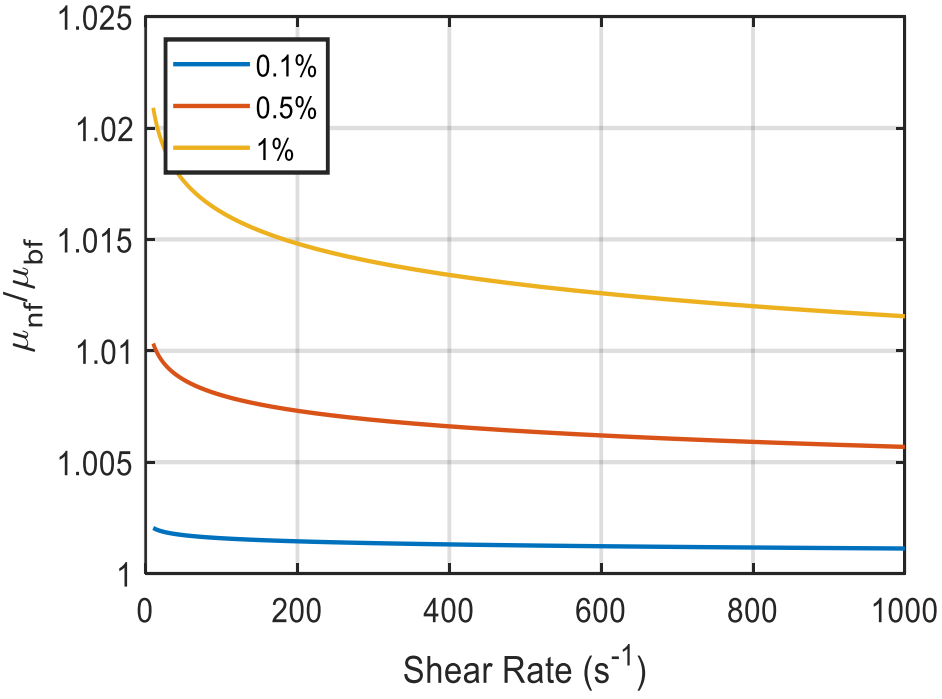

Figure 7. Viscosity ratio indicates shear-thinning behavior at higher nanoparticle concentrations.

The results of the validation, as presented in Table 3, clearly show that there is a high level of agreement between the experimental and numerical results over a wide range of operating conditions. In addition, it is noted that the deviation is within ±8% for all the results, thereby proving the validity of the numerical model. It is noted that the deviation slightly increases with increased velocity and nanoparticle concentration. This can be explained by the increased turbulence, increased particle-particle interactions, and nanoparticle agglomeration, which are not considered in the current model. In conclusion, it is noted that the numerical model is a reliable tool for predicting the heat transfer behavior under jet impingement conditions.

For the purpose of characterizing the rheological behavior of the nanofluid, the experimental results were fitted using the power law model:

$$\tau = K\dot{\gamma}^{n}$$

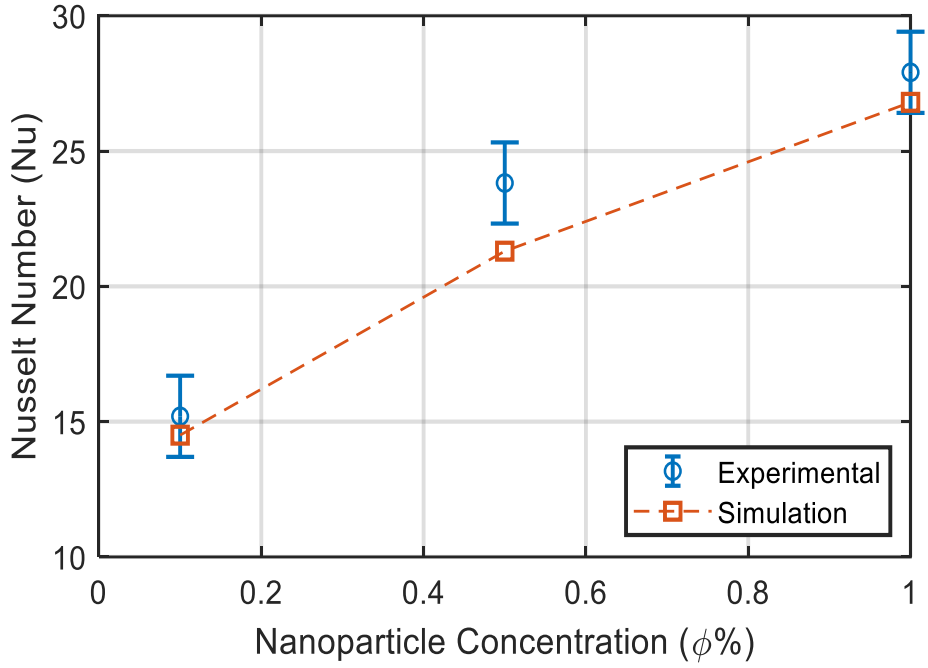

Figure 8. Simulated and experimental Nusselt numbers agree within ±8%, validating the numerical model.

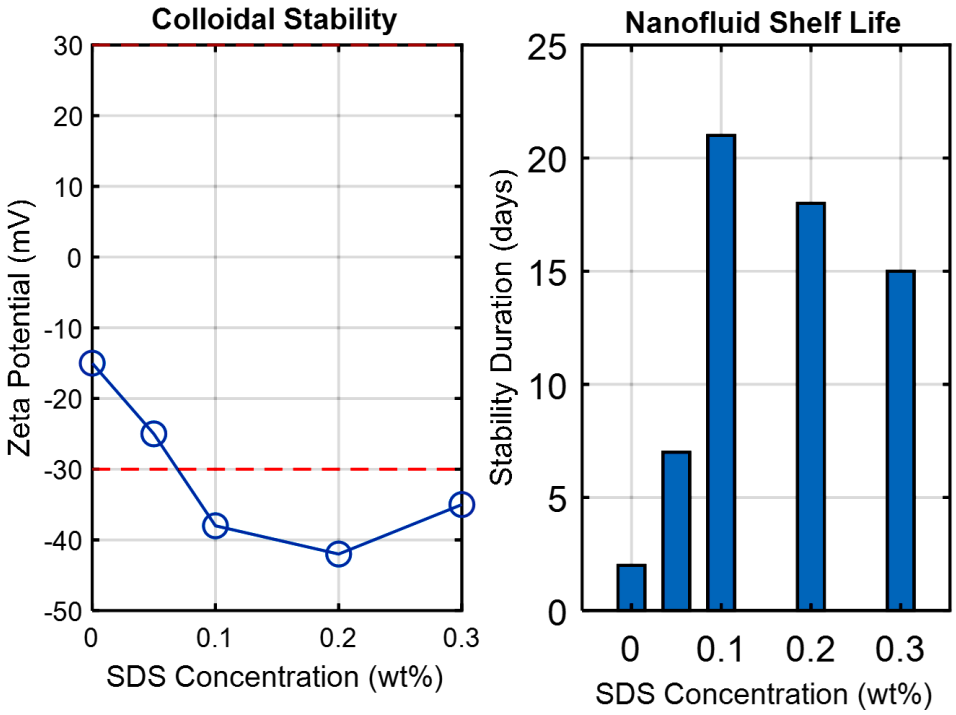

Figure 9. Stability analysis confirms minimal dispersion variation over time using UV–Vis and zeta potential measurements.

Where τ\tauτ is shear stress, γ˙ is shear rate, K is the consistency index, and n is the flow behavior index.

The extracted rheological parameters at different nanoparticle concentrations are summarized in Table 4.

The base fluid has a Newtonian characteristic with a flow behavior index close to unity. With an increase in nanoparticle concentration, there is a gradual reduction in the flow behavior index, indicating a shift to a shear-thinning (pseudo-plastic) fluid characteristic. Non-Newtonian effects start to manifest for a nanoparticle concentration above 0.5% by volume. This can therefore be considered as the threshold for non-Newtonian effects. The consistency index also increases with concentration, indicating a rise in resistance to flow.

Table 3. Validation of Numerical Model Against Experimental Data

Case	Velocity (m/s)	Volume Fraction (%)	Heat Flux (W/cm²)	Nu (Experimental)	Nu (Simulation)	Deviation (%)
1	5	0.1	5	52	50	3.85
2	10	0.5	10	78	74	5.13
3	15	1.0	15	112	105	6.25
4	20	1.0	20	145	136	6.21
5	10	0.1	15	70	67	4.29
6	15	0.5	10	95	90	5.26

Table 4. Power-law Rheological Parameters

Volume Fraction (%)	K (Pa·sⁿ)	n	R²
0 (Base fluid)	0.0010	1.00	0.999
0.1	0.0012	0.98	0.998
0.5	0.0018	0.95	0.997
1.0	0.0026	0.91	0.996

High R^2 values (>0.996) confirm a good fit of the power-law model to the experimental data.

The appearance of non-Newtonian effects has important implications for pumping power. Although thermal performance is enhanced at a higher concentration, there will also be a rise in viscosity and a shift to a shear-thinning characteristic, leading to a possible increase in pressure drop.

3.1 Numerical Implementation

For the numerical simulation, a finite volume method along with a pressure-velocity coupling scheme was used. The governing equations for mass, momentum, and energy conservation were solved for steady-state conditions. For accuracy, second-order schemes for spatial terms in the governing equations were applied. Convergence for the simulation was obtained when the residuals for the continuity, momentum, and energy equations fell below 10^{-6}. Proper boundary conditions for the simulation, such as a uniform velocity inlet, constant heat flux for the target surface, and pressure outlet, were applied. The thermophysical properties of the hybrid nanofluid were included in the simulation, and the values for the thermophysical properties were obtained from experiment.

3.2 Grid Independence Study

Grid independence is checked using three different mesh sizes. This is necessary to ensure that the results are not affected by the mesh size.

Table 5. Grid independence (mesh sensitivity) analysis showing convergence of the predicted average Nusselt number with increasing mesh resolution.

From the results, it is evident that the difference in the Nusselt number between the medium and fine mesh is less than 1%, thereby validating grid independence. Hence, the medium mesh is chosen for all simulations to obtain an optimum balance between computational cost and accuracy. Grid independence is necessary to ascertain that the numerical results are not affected by mesh size. As depicted in Table 5, it is evident that the difference in the calculated average Nusselt number between the medium and fine mesh is less than 1%. Hence, the medium mesh is chosen for all simulations to obtain an optimum balance between computational cost and accuracy.

The improvement in heat transfer and Nusselt number with increasing jet velocity and nanoparticle concentration is in agreement with the previously reported results of nanofluid jet impingment heat transfer. The enhancement in heat transfer with nanoparticle concentration is well established in the field of heat transfer. The addition of nanoparticles to the base fluid is expected to enhance the effective thermal conductivity of the fluid, thereby enhancing convective heat transfer characteristics.

For example, experimental investigations have reported substantial improvement in Nusselt number with increasing nanoparticle concentration in jet impingement heat transfer due to the improvement in thermal transport properties and increased mixing [35].

Table 5. Grid independence (mesh sensitivity) analysis showing convergence of the predicted average Nusselt number with increasing mesh resolution

Mesh Level	Number of Cells	Average Nusselt Number	Deviation (%)
Coarse	45,000	92.5	—
Medium	85,000	95.2	2.9
Fine	130,000	96.1	0.9

Moreover, recent investigations in hybrid nanofluid heat transfer have reported improvement in heat transfer characteristics. The improvement in Nusselt number is reported to be around 15–20%.

Moreover, review articles have established that Reynolds number and nanoparticle concentration are the governing parameters in jet impingement heat transfer, and their increase will result in turbulence and thinner thermal boundary layers, thereby increasing heat transfer coefficient [36]. The results are in agreement with this phenomenon, and increased jet velocities enhance heat transfer due to increased turbulence, resulting in higher heat transfer rates at the stagnation point. The stability of the prepared hybrid nanofluid has been examined through zeta potential and UV-Vis spectrophotometry, and the results confirmed the satisfactory stability of the prepared nanofluid over a 14-day period. The obtained zeta potential values lie in the stable region, i.e., $|\zeta| > 30$ mV, indicating considerable electrostatic repulsion between the dispersed particles and minimal tendency to agglomeration. To ensure the stability of the nanofluid is maintained over the duration of the thermal measurements, the duration and conditions of the jet impingement tests were carefully controlled. This ensured that the total time of the experiments remained within the stability window. During and after the experiments, no visible sedimentation and phase separation were observed. Moreover, to confirm the stability of the nanofluid, the thermophysical properties, i.e., thermal conductivity and viscosity, were re-measured after carrying out the experiments through repeated cycles of heating. Within the bounds of experimental uncertainty, no significant deviation in the thermophysical properties was detected, which further confirms the stability of the nanofluid over the entire period of the experiment. The UV-Vis absorbance measurements, conducted prior to and following the experiments, also confirmed minimal change, indicating the stability of the nanofluid and minimal tendency to agglomeration. By comparing the obtained results, it is observed that the obtained enhancement in heat transfer is within the range of existing results, although some minor discrepancies in the obtained results can be attributed to the specific conditions of the experiments. The enhancement in heat transfer for the jet impingement configuration is attributed to the combined effects of thermophysical and hydrodynamic properties. It is noted from the existing literature that, unlike other conventional flow configurations, the jet impingement configuration has a strong stagnation region, high velocity gradients, and a significantly thinned thermal boundary layer. All these factors contribute to an increase in the local heat transfer coefficient and the overall Nusselt number. However, there is a simultaneous increase in viscosity, particularly for a higher concentration of nanoparticles. This may affect the momentum boundary layer and reduce the flow mobility, resulting in a greater pressure drop and increased pumping power requirement.

Furthermore, the onset of non-Newtonian behavior for a higher concentration of nanoparticles may alter the flow behavior near the wall and affect the turbulence structures in the impinging jets region. To confirm whether a synergistic effect is present in the hybrid nanofluid, the thermal performance has been compared to the expected additive contribution of both nanoparticles [37]. The results show that there is indeed a synergistic effect between Al_2O_3 and Ag nanoparticles, as the measured enhancement in thermal conductivity and Nusselt number is greater than the expected linear combination of both nanoparticles. It is important to note here that the validation of the numerical model has been performed for a relatively simpler case, based on integral heat transfer results such as average Nusselt number. This provides a good indication of thermal performance but may not show detailed flow structures and temperature distribution within the impinging jets region. For further credibility of the numerical model, future work should include validation of results against detailed velocity and temperature fields using sophisticated techniques such as Particle Image Velocimetry (PIV) and infrared thermography. The presence of nanoparticles further enhances this phenomenon by increasing the thermal conductivity and energy transport mechanisms such as microscale conduction and convection, and Brownian motion.

This phenomenon can be explained by the combined effects of both constituents, as silver (Ag) nanoparticles possess a high thermal conductivity, and aluminum oxide (Al_2O_3) provides stability to the mixture by avoiding agglomeration. Nevertheless, at a certain level of concentration, there is a possibility of a rise in viscosity, which might reduce the thermal enhancement. This phenomenon has significant importance for system design. At a high concentration of nanoparticles, a non-Newtonian behavior is observed, in which a decrease in

viscosity is noticed as the shear rate is increased. This phenomenon has significant importance for impinging jets, as a high shear rate near the stagnation region may reduce viscosity, thereby increasing fluid mixing. Nevertheless, at a low shear rate, the apparent viscosity increases, resulting in a rise in pressure drop, thereby increasing energy consumption. Although a rise in nanoparticle concentration results in enhanced heat transfer, a high concentration may lead to a reduction in energy efficiency. Hence, it is necessary to identify an optimum concentration for nanoparticles to enhance heat transfer as well as to avoid a rise in energy consumption.

From an engineering point of view, it is necessary to identify the overall performance of the hybrid nanofluid by optimizing heat transfer enhancement and hydrodynamic penalty. Although a rise in nanoparticle concentration results in enhanced heat transfer, a high concentration may lead to a reduction in efficiency. Hence, there is a possibility of identifying an optimum concentration for nanoparticles to enhance heat transfer as well as to avoid a rise in energy consumption. Moreover, under the conditions of repetitive thermal loading, the long-term viability of the nanofluid is dependent upon the stability and the level of agglomeration. From the results obtained in the present study, it is evident that the hybrid nanofluid is capable of providing an optimal balance between the thermal and flow resistances, thereby ensuring the viability of the hybrid nanofluid for the intended cooling application. Although the stability results are satisfactory in the initial conditions, the possibility of agglomeration under conditions of high shear rates and elevated temperatures must also be taken into consideration. Under the conditions of jet impingment, the nanofluid is subjected to very high shear rates and temperature gradients, which could result in the agglomeration of the nanoparticles over time. The addition of SDS plays a very important role in the stabilization of the hybrid nanofluid by inhibiting the agglomeration of the nanoparticles and ensuring the uniformity of the hybrid nanofluid. However, the addition of surfactants could result in the creation of an interfacial layer around the nanoparticles, thereby affecting the thermal conductivity and the thermal energy transfer from the nanoparticles to the fluid. This could result in the reduction of the thermal conductivity enhancement. However, the improved stability of the hybrid nanofluid by the addition of SDS is beneficial in the present study, as the negative effects are compensated by the positive effects. In the present study, it is evident that the addition of SDS is beneficial, as the negative effects are compensated by the positive effects. Moreover, the sedimentation and the changes in thermal performance were not evident in the present study, and the nanofluid is stable over the duration of the study. However, the possibility of microstructural changes cannot be ruled out.

Future work will include post-experimental characterization, such as scanning and transmission electron microscopy and particle size analysis, to evaluate the aggregation behavior of the hybrid nanofluid after long-term thermal and hydrodynamic treatment. This will also add to the reliability of hybrid nanofluid in cooling applications. Thus, even though this study shows the promise of using hybrid nanofluid in thermal applications, further research is necessary to make it cost-effective and assess the environmental impact before it is taken to industrial applications.

4. Conclusion

This study sought to evaluate the thermophysical properties and heat transfer characteristics of Al_2O_3–Ag hybrid nanofluid, as well as the predictive modeling of the heat transfer characteristics of this nanofluid under jet impingement conditions. As expected, the experiment revealed some improvement in thermal conductivity and changes in viscosity, including the appearance of non-Newtonian behavior at high concentrations. The experiment also showed that the heat transfer characteristics of Al_2O_3–Ag hybrid nanofluid under jet impingement conditions are enhanced, as revealed by the increase in heat transfer coefficient and Nusselt number with increasing nanoparticle concentration and jet velocity.

The numerical model developed in this experiment showed satisfactory agreement with the experimentally obtained data, thereby validating the ability of this numerical model to predict the heat transfer characteristics of Al_2O_3–Ag hybrid nanofluid within acceptable limits of deviation. The results of this experiment also showed that, even as the heat transfer characteristics of Al_2O_3–Ag hybrid nanofluid are enhanced, the viscosity of this fluid also increases, thereby requiring an optimum range of operation to be established.

From the results of this experiment, it is evident that the objectives of this research have been achieved, and it is now possible to assert that it is possible to enhance the jet cooling characteristics of this fluid.

References

[1] Q. Nguyen, C.L. Nelson, D.S. Drew, Jet Impingement Cooling with Multi-Stage Ducted Electroaerodynamic Actuators. Applied Thermal Engineering, 296, (2026) 130770. https://doi.org/10.1016/j.applthermaleng.2026.130770

[2] I. Lee, H. Cho, S. Kim, J. Kim, Y. Nam, High Efficiency Single and Multi-Phase Direct Liquid Jet-Impingement Cooling for Heterogeneous Packaging. Energy Conversion and

Management, 348(P-B), (2026) 120665. https://doi.org/10.1016/j.enconman.2025.120665

[3] Q. Zhang, P. Chen, X. Zhao, X. Yu, A.R.B.M. Yusoff, Y. Yu, P. Gao, Thermal Management of Perovskite Solar Cells. ChemSusChem, 19(1), (2026) e202501649. https://doi.org/10.1002/cssc.202501649

[4] P. Barmavatu, J. Heeraman, M.K. Das, R.V. Mangalaraja, M. Srinivasnaik, Synergistic Integration of Micro-Channels and Thermal Storage Systems for Energy Efficiency Enhancement in Heat Transfer Applications-A Critical Review. Journal of Thermal Analysis and Calorimetry, 151(2), (2026) 1097-1119. https://doi.org/10.1007/s10973-025-15165-w

[5] J. Heeraman, Introduction to Heat Transfer in Sustainable Energy Systems. In Artificial Intelligence and Machine Learning in Heat Transfer Optimization for Sustainable Energy Systems, CRC Press, (2026) 1-22.

[6] Y. Ying-de, S. Heng-lin, N. Ya-shan, L. Shi-jie, Z. Wen-heng, Z. Shao-heng, Q. Ling-yun, H. Jin-jie, H. Xin-hao, Tube-Side Flow Resistance and Enhanced Heat Transfer for a Novel Twisted Elliptical Tube Double-Pipe Heat Exchanger. International Journal of Thermal Sciences, 225, (2026) 110793. https://doi.org/10.1016/j.ijthermalsci.2026.110793

[7] M.M. Nour, M.A. Tony, H.A. Nabwey, Nanomaterials and Nanofluids for Environmental Applications: A Comprehensive Review. Journal of Engineering, 2026(1), (2026) 3370145. https://doi.org/10.1155/je/3370145

[8] K. Deshpande, Foundations and Applications of Ionic Liquids, Nanofluids, Nanomaterials, and Nanotechnology: A Comprehensive Introduction. In Ionic Liquids, Nanofluids and Nanotechnology: Innovations, Applications and Sustainability, Springer Nature Switzerland, Cham, 42 (2026) 81-107. https://doi.org/10.1007/978-3-032-04008-4_4

[9] M. Manimaran, M.N. Norizan, M.H.M. Kassim, M.R. Adam, N. Abdullah, M.N.F. Norrrahim, E. Bayraktar, Stability and Thermal Conductivity of Water-Based Hybrid Nanofluids using Oil Palm Biomass Cellulose Nanoparticles and Metal Oxide Nanoparticles. Polimery, 71(3), (2026) 187-202. https://doi.org/10.14314/polimery.2026.3.5

[10] S. Cai, J. Fan, J. Wang, Y. Ma, Y. Xiao, S. Cheng, G. Lv, X. Zeng, X. Zeng, J. Xu, L. Ren, Y. Yao, X. Zeng, X. Zeng, R. Sun, Yield-Stress Composite Fluids with High Thermal Conductivity and Tunable Rheology via Hierarchical Filler Architecture. Small, 22(15), (2026) e13010. https://doi.org/10.1002/smll.202513010

[11] S. Samsami, E. Jacob, N. Nguyen, K.C. Tam, M. Kamkar, CNT Aqueous Sonogels: Rapid, Green, Rheology-Tunable Inks for Hybrid Formative-Additive Manufacturing Yielding Multifunctional Robust Cryogels. Carbon, 253, (2026) 121372. https://doi.org/10.1016/j.carbon.2026.121372

[12] A. Aslam, Y. Hu, S. Wakeel, Y. Zheng, R. Zhai, J. Zhang, Functional Polymers via Heterogeneous Polymerization for Oilfield Application. ChemistrySelect, 11(12), (2026) e07394. https://doi.org/10.1002/slct.202507394

[13] M. Sanches, G. Marseglia, A.P. Ribeiro, A.L. Moreira, A.S. Moita, Nanofluids Characterization for Spray Cooling Applications. Symmetry, 13(5), (2021) 788. https://doi.org/10.3390/sym13050788

[14] M. Malý, A.S. Moita, J. Jedelsky, A.P.C. Ribeiro, A.L.N. Moreira, Effect of Nanoparticles Concentration on the Characteristics of Nanofluid Sprays for Cooling Applications. Journal of Thermal Analysis and Calorimetry, 135(6), (2019) 3375-3386. https://doi.org/10.1007/s10973-018-7444-z

[15] M. Asim, F.R. Siddiqui, Hybrid Nanofluids—Next-Generation Fluids for Spray-Cooling-based thermal Management of High-Heat-Flux Devices. Nanomaterials, 12(3), (2022) 507. https://doi.org/10.3390/nano12030507

[16] A. Mirahmad, R. Shankar Kumar, B. Pato Doldán, C. Prieto Rios, J. Díez-Sierra, beyond Thermal Conductivity: A Review of Nanofluids for Enhanced Energy Storage and Heat Transfer. Nanomaterials, 15(4), (2025) 302. https://doi.org/10.3390/nano15040302

[17] A. Mund, B. Pattanayak, Thermal Performance Analysis of Nanofluid Spray Impingement in Heat Transfer Applications. Sadhana, 51(2), (2026) 79. https://doi.org/10.1007/s12046-025-03033-0

[18] W. Bunpheng, R. Dhairiyasamy, D. Varshney, S. Singh, C.K. Chan, E. Murugesan, Multi-Objective Engineering Optimization of Nanofluid Coolants in Compact Slotted Pin-Fin Heat Exchangers. International Journal of Thermofluids, 32, (2026) 101588. https://doi.org/10.1016/j.ijft.2026.101588

[19] M. Ayman-Mursaleen, S.T. Saeed, S.M. Almohammadi, K. Arif, M. Imran, A Deep Neural Network Model for Heat Transfer in Darcy–Forchheimer Hybrid Nanofluid Flow with Activation Energy. Scientific Reports, 16(1), (2026) 8339. https://doi.org/10.1038/s41598-026-39536-x

[20] H. Alshehemah, S.A. Ebrahim, S. Mukherjee, B.T. Balakrishnan, A.M. Bahman, Rheological behavior and Stability of Mono and Hybrid Carbon Nanotube—Titanium Dioxide Nanofluids in Ethylene Glycol and Water Basefluids. Journal of Molecular Liquids, 447, (2026) 129402. https://doi.org/10.1016/j.molliq.2026.129402

[21] B.E. Hadoui, Y. Ighris, M. Kaddiri, J. Baliti, Thermal Performance of Non-Newtonian Water–Ethylene Glycol Nanofluids in Enclosed Natural Convection. In Engineering Materials, (2026) 127-142. https://doi.org/10.1007/978-3-032-10069-6_9

[22] S. Zainon, W. Azmi, Recent Progress on Stability and Thermo-Physical Properties of Mono and Hybrid towards Green Nanofluids. Micromachines, 12(2), (2021) 176. https://doi.org/10.3390/mi12020176

[23] N.K. Jain, D. Paliwal, P. Jain, Characterization and Effectiveness Analysis of Ternary Organic Eutectic Mixture/Hybrid-Nanoparticles based Phase Change Material for Cold Storage Applications. Physica Scripta, 100(1), (2025) 015016. https://doi.org/10.1088/1402-4896/ad9873

[24] S. Kalsi, S. Kumar, A. Kumar, T. Alam, A. Sharma, A.S. Yadav, A Review on Hybrid Nanofluids for Heat Transfer: Advancements, Synthesis, Challenges and Applications. Discover Applied Sciences, 7(7), (2025) 698. https://doi.org/10.1007/s42452-025-07141-8

[25] V.V. Wanatasanapan, M.Z. Abdullah, P. Gunnasegaran, Effect of TiO_2-Al_2O_3 Nanoparticle Mixing Ratio on the Thermal Conductivity, Rheological Properties, and Dynamic Viscosity of Water-based Hybrid Nanofluid. Journal of Materials Research and Technology, 9(6), (2020) 13781-13792. https://doi.org/10.1016/j.jmrt.2020.09.127

[26] N. Nayebpashaee, (2025). Experimental Investigation of a Novel Al_2O_3–TiO_2–CuO–Fe_3O_4/water–EG Quadri Hybrid Nanofluid: Effects of Temperature and Nanoparticle Concentration on Thermophysical Properties. https://doi.org/10.21203/rs.3.rs-8024960/v1

[27] J. Syed, Enhancement of Heat Transfer using Water/Graphene Nanofluid and the Impact of Passive Techniques—Experimental, Numerical, and ML Approaches. Energies, 18(1), (2024) 77. https://doi.org/10.3390/en18010077

[28] M. Benkhedda, T. Boufendi, S. Touahri, Laminar Mixed Convective Heat Transfer Enhancement by using Ag-TiO_2-Water Hybrid Nanofluid in a Heated Horizontal Annulus. Heat and Mass Transfer, 54(9), (2018) 2799-2814. https://doi.org/10.1007/s00231-018-2302-x

[29] B.A.A. Silva, (2018). Rheological Characterization and Modelling of CNT nanofluids (Doctoral dissertation, Universidade de Aveiro (Portugal)).

[30] C.N. Minh, Heat Transfer Enhancement Using Al_2O_3, CuO, and Hybrid Al_2O_3–CuO Nanofluids in Water and Ethylene Glycol–Water Mixtures in an Automotive Radiator. International Journal of Heat & Technology, 43(4), (2025) 1429-1438. https://doi.org/10.18280/ijht.430420

[31] M. Manimaran, M.N. Norizan, M.H.M. Kassim, M.R. Adam, N. Abdullah, M.N.F. Norrrahim, Critical review on the Stability and Thermal Conductivity of Water-based Hybrid Nanofluids for Heat Transfer Applications. RSC advances, 15(18), (2025) 14088-14125. https://doi.org/10.1039/D5RA00844A

[32] P. Selvan, D. Jebakani, K. Jeyasubramanian, D.J.J. Jebaraj, Enhancement of Thermal Conductivity of Water based Individual and Hybrid SiO_2/Ag Nanofluids with the usage of Calcium Carbonate Nano Particles as Stabilizing Agent. Journal of Molecular Liquids, 345, (2022) 117846. https://doi.org/10.1016/j.molliq.2021.117846

[33] L. Yu, Y. Bian, Y. Liu, X. Xu, Experimental Investigation of Rheological Properties of low Concentrated TiO_2/Water and MWCNT-TiO_2/Water Hybrid Nanofluids. Heat and Mass Transfer, 56(8), (2020). 2545-2556. https://doi.org/10.1007/s00231-020-02868-z

[34] F. Alshehri, J. Goraniya, M.L. Combrinck, Numerical Investigation of Heat Transfer enhancement of a Water/Ethylene Glycol Mixture with Al_2O_3–TiO_2 Nanoparticles. Applied Mathematics and Computation, 369, (2020) 124836. https://doi.org/10.1016/j.amc.2019.124836

[35] P.K. Tyagi, R. Kumar, P.K. Mondal, A review of the State-Of-The-Art Nanofluid Spray and Jet Impingement Cooling. Physics of Fluids, 32(12), (2020) 121301. https://doi.org/10.1063/5.0033503

[36] B.A. Shirvani, J. Sodagar, F. Eynijengheshlaghi, A. Arabkoohsar, Numerical Investigation of Nanoparticles Shape Impacts on Thermal Energy Transfer and Flow Features of nanofluid Impingement Jets. Journal of Energy Resources Technology, 143(11), (2021) 112002. https://doi.org/10.1115/1.4049737

[37] X. Wu, P. Moin, Transitional and Turbulent Boundary Layer with Heat Transfer. Physics of Fluids, 22(8), (2010) 085105. https://doi.org/10.1063/1.3475816

Authors Contribution Statement

Ammar F. Abdulwahid: Conceptualization, Methodology, Validation, Formal Analysis, Writing - Original Draft. Hayder S. Al-Madhhachi: Methodology, Investigation, Data Curation. Firas Thair Al-Maliky: Data Curation, Writing - Review & Editing. Muthanna Abd Ali Awad Madhhachi: Data Curation, Writing - Review & Editing. All the authors read and approved the final version of the manuscript.

Funding

The authors declare that no funds, grants or any other support were received during the preparation of this manuscript.

Competing Interests

The authors declare that there are no conflicts of interest regarding the publication of this manuscript.

Data Availability

The data supporting the findings of this study can be obtained from the corresponding author upon reasonable request.

Has this article screened for similarity?

Yes